frontiers | Frontiers in Earth Science

ORIGINAL RESEARCH
published: 06 July 2022
doi: 10.3389/feart.2022.933058

# Hydrocarbon Accumulation Mechanism of Ordovician in the Halahatang Area, Tarim Basin —Evidence From Organic Geochemistry

*Fei Huo[1,2], Xingzhi Wang[1,2], Luping Li[3,4], Xin Luo[3,4]*, Xiyan Yang[1,2], Chen Shen[3,4]*, Liang Li[3,4], Yunbo Ruan[3,4] and Huiwen Huang[3,4]**

*[1]State Key Laboratory of Oil and Gas Reservoir Geology and Exploitation, Southwest Petroleum University, Chengdu, China, [2]School of Geoscience and Technology, Southwest Petroleum University, Chengdu, China, [3]State Key Laboratory of Oil and Gas Reservoir Geology and Exploitation, Chengdu University of Technology, Chengdu, China, [4]Institute of Sedimentary Geology, Chengdu University of Technology, Chengdu, China*

OPEN ACCESS

***Edited by:***
*Junhui Wang,*
*China University of Petroleum, China*

***Reviewed by:***
*Zheng Cao,*
*Chongqing University of Science and Technology, China*
*Lianchao Luo,*
*University of Florence, Italy*
*Kelai Xi,*
*China Univeristy of Petroleum, China*

****Correspondence:***
*Xin Luo*
*747210227@qq.com*
*Chen Shen*
*369688809@qq.com*
*Huiwen Huang*
*573412784@qq.com*

***Specialty section:***
*This article was submitted to Structural Geology and Tectonics, a section of the journal Frontiers in Earth Science*

***Received:*** *30 April 2022*
***Accepted:*** *27 May 2022*
***Published:*** *06 July 2022*

***Citation:***
*Huo F, Wang X, Li L, Luo X, Yang X, Shen C, Li L, Ruan Y and Huang H (2022) Hydrocarbon Accumulation Mechanism of Ordovician in the Halahatang Area, Tarim Basin—Evidence From Organic Geochemistry. Front. Earth Sci. 10:933058. doi: 10.3389/feart.2022.933058*

As an important oil and gas-bearing area in the Tarim Basin, the Halahatang Area has great potential for resource exploration. However, the research on oil and gas sources and the filling period of the Lower Paleozoic Ordovician is still limited. In this study, the organic geochemical analysis of source rocks, the simulation technology of hydrocarbon generation evolution basin, the distribution characteristics of fluid inclusions, and the measurement of uniform temperature are used and combined with the stable isotope of natural gas and the characteristics of oil-source biomarkers, and the process of oil and gas accumulation is restored. The results show that: ①The Cambrian source rock is the main contributor to Ordovician crude oil in the Halahatang Area, and its crude oil shows the characteristics of lightweight, rich chain hydrocarbons, and poor aromatic hydrocarbons. The composition of $C_7$ compound shows the advantage of n-heptane, which belongs to type I kerogen. The biomarker compounds show the characteristics of high content of long-chain tricyclic terpane and high Ts/Tm values, and the crude oil is considered to be a highly mature sapropelic kerogen source oil. ②The carbon isotopes of methane and ethane of Ordovician natural gas in the Halahatang Area are light (from −35.6 to −29.5‰), showing obvious characteristics of sapropelic gas. ③There are three stages of the oil and gas accumulation process in Ordovician reservoirs in the Halahatang Area. In the middle and late Caledonian periods, the source rock reached the hydrocarbon generation threshold and began to generate oil. The late Hercynian period was the main accumulation period, and the Himalayan period was dominated by dry gas filling. ④The crude oil generated in the Middle-Late Caledonian periods migrated along the faults and conductive layers and finally accumulated in the high parts of the structure in the north. The migration of oil and gas in the late Hercynian period was limited by the bitumen produced by early biodegradation. Since the asphalt plugging condensate gas has almost failed to cause gas invasion from the reservoir, the Ordovician reservoir still maintains the characteristics of crude oil-associated gas, forming an oil and gas reservoir with a gas cap.

**Keywords: halahatang area, stable isotopes, biomarkers, oil-gas source correlation, fluid inclusions, accumulation model**

## 1 INTRODUCTION

The Tarim basin is a typical multi-stage structural superimposed basin in western China, with abundant oil and gas resources and great potential for exploration and development. In 2009, after the high-yield industrial oil and gas flow was obtained in the Ordovician Yijianfang Formation of well Ha 6C in Halahatang Oilfield (Cheng et al., 2013), blocks such as Xinken and Repu were successively explored and developed, with oil and gas geological reserves reaching 100 million tons. The Halahatang Area has become an emerging key exploration block in the North Tarim uplift of the Tarim Basin. However, the exploration of Ordovician oil and gas in the Halahatang Area is restricted by many factors, such as multi-stage structural superposition, deep burial depth of deep marine carbonate strata, reservoir densification, strong reservoir heterogeneity, and insufficient understanding of hydrocarbon accumulation conditions. To solve the above problems, a large number of studies have been carried out in this area, but the source rock and its hydrocarbon accumulation period have been controversial (Zhao et al., 2008a; Zhao et al., 2008b; Li et al., 2010; Li et al., 2010b; Li et al., 2015). Most studies tend to advocate that the main source rocks in the Halahatang Area are Cambrian-Lower Ordovician source rocks and Middle-Upper Ordovician source rocks (Zhang et al., 2013; Zhu et al., 2013; Anlai et al., 2020; Wu et al., 2020). For the study of hydrocarbon accumulation age, previous studies have obtained different understandings by means of the thermal evolution history of source rocks, geochemical characteristics of crude oil and inclusions, and homogenization temperature analysis (Li et al., 2010; Zhang et al., 2011; He et al., 2022). For example, Chen et al. (2014) believed that the Ordovician reservoirs in Tahe Oilfield had three stages of oil and gas accumulation: Middle Carboniferous–Early Triassic, Cretaceous–Early Paleogene, and Paleogene–Neogene. Chang et al. (2015) believed that there were two stages of oil and gas accumulation: Late Carboniferous–Early Devonian and Neogene.

The authors believe that the hydrocarbon inclusion results need to be combined with the geochemical characteristics of total hydrocarbons in order to better understand oil and gas accumulation in the Halahatang Area (Zhu et al., 2021). Therefore, under the condition that the oil and gas exploration of the Ordovician in the Halahatang Area has multi-factor constraints, on the basis of previous research results, this study uses organic geochemical analysis of source rocks and hydrocarbon evolution basin simulation technology, fluid inclusion distribution characteristics, and homogenization temperature measurement. On the basis of the regional tectonic setting, combined with the stable isotope of natural gas and the characteristics of oil source biomarkers, the sources of oil and gas, oil and gas accumulation period, and favorable oil and gas accumulation conditions of the Ordovician in the Halahatang area are clarified, and the process of oil and gas accumulation is restored. It provides an important basis for carbonate oil and gas exploration in the Halahatang area of the Tarim Basin.

## 2 GEOLOGICAL SETTING

The Halahatang area is located in the middle of the North Tarim uplift in the Tarim Basin where the Luntai uplift is located in the north, the North depression is located in the south, the Yingmaili low uplift in the west, and the Lunnan low uplift in the east (Zhu et al., 2011), and its area is about 4,000 km$^2$. The Ordovician in the Harahatang area can be divided into the Upper Sangtamu Formation ($O_3s$), Lianglitage Formation ($O_3l$), Tumuxiuke Formation ($O_3t$), Middle Yijianfang Formation ($O_2y$), and Middle-Lower Yingshan Formation ($O_{1-2}y$). The Sangtamu Formation, Lianglitage Formation, and Tumuxiuke Formation of Upper Ordovician were eroded from south to north in turn, and the Silurian Kepingtage Formation was covered on the buried hill of Yijianfang Formation of Ordovician in the north (Zhang et al., 2012; Zhang et al., 2014). The Middle Ordovician Yijianfang Formation~the upper part of the Ying 1 Member of the Middle-Lower Ordovician Yingshan Formation is the main oil-bearing stratum (**Figure 1**). The reservoir rocks of the Middle Ordovician Yijianfang Formation are mainly composed of bright crystal sand-dust limestone, bright crystal sand-gravel limestone, and bright crystal oolitic limestone. The lithology of Ying 1 Member reservoir in Yingshan Formation is mainly composed of bright crystal lithic limestone, lithic argillaceous limestone, and argillaceous limestone. The reservoir space types are mainly matrix pores, dissolution pores, and fractures, and the reservoir heterogeneity is strong (Shen et al., 2007; Zhang et al., 2014). According to the structural buried depth of the Ordovician reservoir, the combined characteristics of the overlying strata, and the oil and gas properties, the Halahatang area was divided into three regions from north to south: the northern buried hill area, the middle slope transition area, and the southern deep-buried area (Li et al., 2010). The strata in the northern buried hill area were eroded and lacked of upper Ordovician. The Kepingtage Formation of Silurian in Qigujing area directly covered Yijianfang Formation as a caprock. The buried depth of the reservoir is 6,500–6,700 m (the ground elevation is about 960 m), and the oil and gas are mainly distributed in Yijianfang Formation and Ying 1 Member. To the south of the slope transition zone, all strata are well developed. The cap rocks are mainly the dense marl and mudstone of the Tumu shock group, Lianglitage Formation, and Sangtamu Formation of the Upper Ordovician. The reservoirs are the Yijianfang Formation and the upper part of the first member of Yingshan Formation of the Ordovician. The oil and gas are distributed in the range of 0–100 m from the top of Yijianfang Formation. Oil and gas are occasionally found in Lianglitage Formation, and the buried depth of the reservoir is 6,600–7,000 m. The burial depth of reservoirs in the deeply

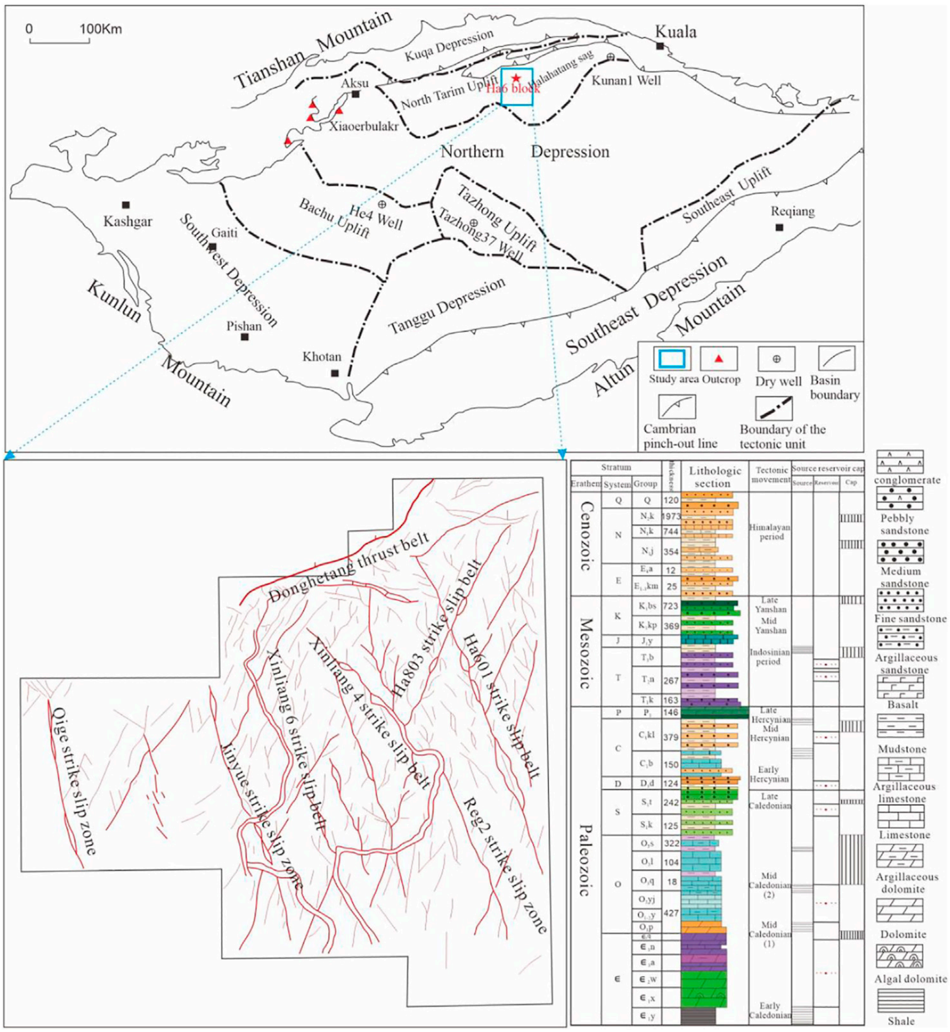


**FIGURE 1 |** Outline map of Ordovician faults in the 3D area of the Liulian block of Halahatang (modified from Li et al., 2021).

buried area in the south is large, mostly below 7,000 m, and the oil and gas are mainly produced in the Yijianfang Formation and the upper part of the first member of Yingshan Formation.

The Halahatang area in the North Tarim has experienced multiple tectonic movements (Ni et al., 2009; Zhang et al., 2012). In the Cambrian-Ordovician, due to the plate tectonic activity of the northern margin of the Tarim plate, the intra-platform uplift belt began to develop in the northern Tarim area. By the end of the Ordovician, the unified North Tarim uplift belt was initially formed with the closure of Ku-Man aulacogen. In the Silurian -Devonian, the North Tarim uplift inherited development, while the Lunnan and Yingmaili areas were further uplifted. In the late Devonian, the North Tarim uplift formed a large-scale erosion area, and the southern part eventually formed a "triconvex" structure pattern. In the Late Carboniferous-Triassic, thrust nappe structures and giant left-lateral strike-slip structural deformation zones dominated by Xinhe-Erbatai, Yingmaili, Lunnan, and Kuerle-Kongquehe slopes were developed in the northern Tarim Basin. Since the Neogene, due to the continuous strong subsidence of the Kuche Depression, the northern Tarim Basin has gradually become the front uplift and foreland slope of the Kuche regenerative Foreland Basin, and the Upper Paleozoic and Mesozoic were tilted, and together with the Cenozoic, it was a large monocline with an overall north dip, and the current tectonic pattern of the Halahatang area was formed (Zhang et al., 2012; Yan et al., 2015).

## 3 SAMPLES AND ANALYTICAL METHODS

### 3.1 Sample Preparation

In this study, Ordovician and Cambrian source rock samples were collected from Well Tazhong 37 and Well He 4, respectively. The crude oil and natural gas samples were taken from the Ha 6 structure, the Xinken structure, and the Repu structure in the Halahatang area. The asphaltenes of the crude oil and the source rocks were separated by petroleum ether (60 ml), followed by further separation of components using silica gel and an alumina column. Separation of saturated hydrocarbons, aromatic hydrocarbons, and non-hydrocarbon components using petroleum ether, dichloromethane, and petroleum ether (2:1, 50 ml) and dichloromethane/methanol (7:1, 40 ml), respectively. Saturated and aromatic hydrocarbon fractions were analyzed with biomarkers using gas chromatography (GC-FID) and mass spectrometry (GC-MS), and carbon isotopes were determined.

## 3.2 GC-FID and GC-MS

Gas chromatography-mass spectrometry analysis: The source rock samples were ground to below 120 mesh as required and then extracted by Soxhlet extraction for 72 h, and an open silica column was used to separate saturated hydrocarbons, aromatic hydrocarbons, and non-hydrocarbon components. GBT30431-2013 was used as the standard. Analysis of whole oil and saturated fractions extracted from source rock and crude oil samples using an Agilent 6890 N GC and MAT 252 MS combined test system equipped with an HP-5MS fused silica capillary column (60 m × 0.25 mm × 0.25 μm), with the carrier gas as helium. The oven temperature was initially 50°C for 1 min, then increased to 320°C at a rate of 4°C/min and held for 25 min. Analysis of n-alkanes and isoprenoids based on total ion chromatography (TIC), identification of terpanes using the m/z191 mass spectrum, and interpretation of steranes based on the m/z217 mass spectrum, calculation of biomarker values based on peak areas.

## 3.3 Stable Carbon Isotope

The stable carbon isotope of crude oil was analyzed by the FLASH 2000EA-MAT 253 IRMS stable isotope mass spectrometer. The crude oil sample was dissolved by dichlorotoluene, and the combustion temperature was initially set to 950°C and gradually adjusted to 250°C. Liquid nitrogen was employed for cooling, purification, and collection. Finally, the value of carbon isotope was calibrated with respect to Pee Dee Belemnite (the error does not exceed 0.1‰) to obtain accurate analysis results.

## 3.4 Gas Components and the Isotope of Natural Gas

Natural gas composition analysis was performed using an Agilent GC6890N gas chromatograph with helium as the carrier gas and a dual TCD detector. The determination of carbon and hydrogen isotopes of natural gas was completed on a Finnigan MAT 252 mass spectrometer. The carbon isotope value was compared with the GBW04405 reference, giving the value relative to the PDB with a standard deviation of ±0.04‰. The analysis of hydrogen isotopes used the value of VSMOW to calibrate the experimental results with a standard deviation of ±0.3‰. The analysis of light hydrocarbons (C5-C8) in natural gas was performed on HP5890IIgas chromatograph with HP-PONA capillary column (50 m × 0.2 mm × 0.5 μm) and helium as carrier gas. The content of light hydrocarbons in natural gas is generally relatively low, but the analysis of light hydrocarbons can be carried out by direct injection of natural gas. The injection volume was generally 10–15 ml, and the light hydrocarbons were enriched by a liquid nitrogen cold trap before the chromatographic column for 5 min. In order to detect as many light hydrocarbon components as possible, the initial temperature of the chromatographic heating program was kept to 35°C for 25 min. Then, the temperature was programmed at 1.5°C/min to 70°C, 3°C/min to 160°C, and 5°C/min to 280°C, and lastly held for 20 min. The injector temperature is 120°C and the FID detector temperature was 320°C.

## 3.5 Fluid Inclusion Thermometry

The analysis of fluid inclusions was performed using a Leica D MRX HC microscope, and the microscopic temperature measurement of fluid inclusions using the Linkam THMSG 600 system with a resolution of about 0.1°C. When the temperature testing varies from 180 to 600°C, and with the test conditions of 25°C temperature and 35% humidity, the heating temperature error is about 1°C, and the cooling temperature measurement error of about 0.1°C.

# 4 RESULTS

## 4.1 Geochemical Characteristics of Source Rocks

### 4.1.1 Carbon Isotope Characteristics of Kerogen

The kerogen carbon isotope values of Cambrian source rocks in the Tarim Basin are lower than those of Upper Ordovician source rocks. The former are mainly distributed in −35.6 ~ −29.5‰, and the latter are mainly distributed in −31.29 ~ −29.69‰ (**Figure 2**), which is mainly related to biological evolution. Cambrian source rocks and Ordovician source rocks are close in age. Although the carbon isotope age effect indicates that the carbon isotope of oil generated from Cambrian source rocks is lighter than that of oil generated from Ordovician source rocks, the specific value is not clear.

### 4.1.2 Characteristics of Biomarkers

The content of tricyclic terpanes in Cambrian-Lower Ordovician source rocks is high, and the content of $C_{24}$ tetracyclic terpanes is low. The content of $C_{28}$ and $C_{29}$ long-chain tricyclic terpanes is high, and the content of gammacerane is high, which is almost equal to or more than that of $C_{31}$ hopane. For the content of sterane, it shows the distribution characteristics of $C_{29} > C_{28} > C_{27}$. Some samples show the distribution characteristics of $C_{29} > C_{27} > C_{28}$, but the content of $C_{28}$ sterane is still relatively high. In addition, the content of rearranged sterane is low (**Figure 3**; **Table 1**).

The Upper Ordovician limestone source rocks are collected from wells Tazhong 37 and so on. These wells do not have or only have a small amount of oil and gas in the Upper Ordovician limestone and are far from the reservoir site. These limestone source rocks have relatively high organic matter abundance, which is representative of the Upper Ordovician marl source rocks.

Compared with the Cambrian-Lower Ordovician source rocks, the marl source rocks of the Upper Ordovician have lower tricyclic terpanes, $C_{28}$ and $C_{29}$ long-chain tricyclic terpanes, gammacerane, and Ts/Tm ratio, indicating that the

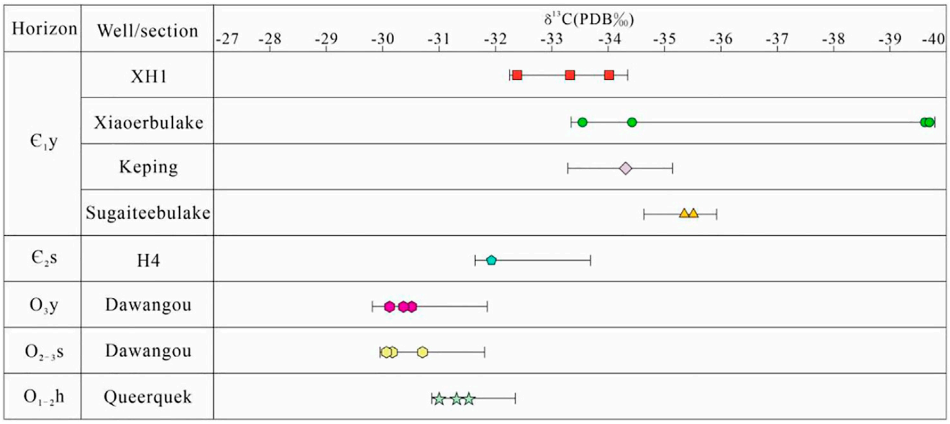


**FIGURE 2 |** Isotope distribution of kerogen in Cambrian-Ordovician source rocks in the Tarim Basin.

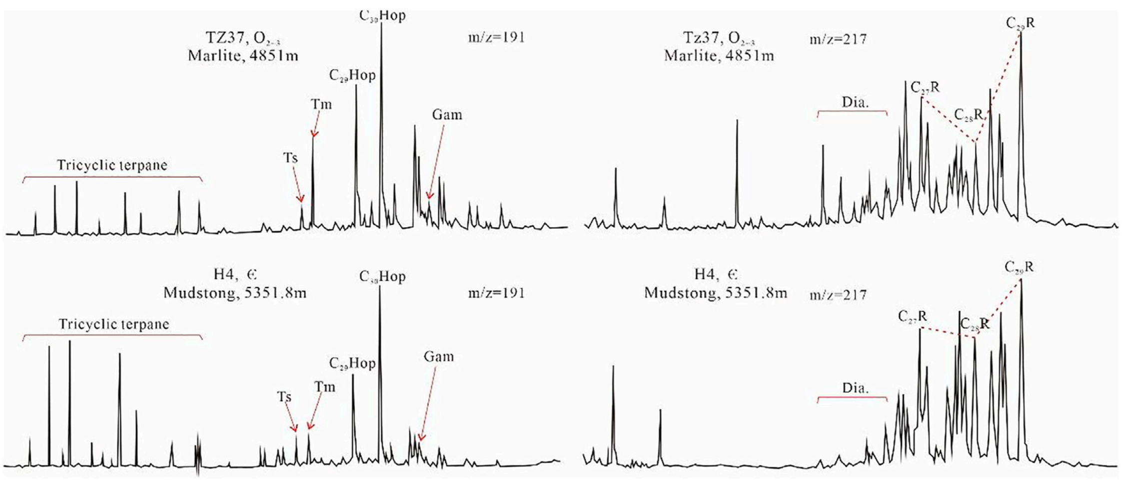


**FIGURE 3 |** Chromatograms of steranes and terpanes of Cambrian-Lower Ordovician and Middle-Upper Ordovician source rocks in well Tazhong 37 and well He 4.

**TABLE 1 |** Comparison of source rock biomarking parameters between middle and lower cambrian—lower ordovician and upper ordovician.

| Source rock biomarker parameter | Cambrian-lower ordovician source rocks | Upper ordovician source rocks |
|---|---|---|
| Gammacerane/$C_{31}$ hopane | high | low |
| $C_{28}$ sterane | high | low |
| $C_{27}$, $C_{28}$, $C_{29}$ sterane | $C_{27} < C_{28} < C_{29}$ or $C_{27} > C_{28} < C_{29}$ | $C_{27} > C_{28} < C_{29}$ |
| tricyclic terpenes/hopane | high | low |
| rearranged sterane/regular sterane | low | high |
| long-chain tricyclic terpane $C_{28}$, $C_{29}$ | high | low |
| $C_{31}/C_{30}$ hopane | low | high |

Cambrian source rocks have higher maturity. Both of their distributions of steranes show a typical "V" shaped distribution, although $C_{29} > C_{27} > C_{28}$ also appears. However, the content of $C_{28}$ sterane in the Upper Ordovician is lower than that in Cambrian-Lower Ordovician source rocks. In addition, the content of rearranged sterane is higher than that of Cambrian-Lower Ordovician source rocks (**Figure 3**).

Oils generated from Cambrian source rocks contain gammacerane in the early stages, but the content of gammacerane is low during and after the peak of oil generation. The abundance of

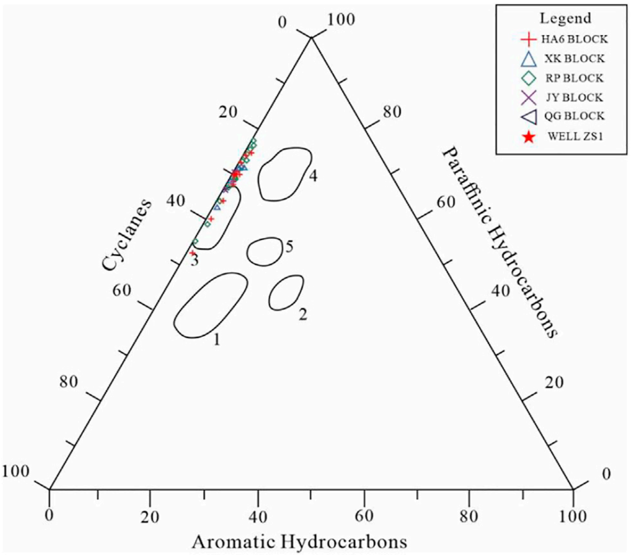


**FIGURE 4 |** Triangular plot of $C_4$-$C_7$ light hydrocarbon family components of Halahatang Ordovician crude oil. Note: Regions 1 and 2: humic kerogen; Regions 3 and 4: sapropelic kerogen; Region 5: mixed kerogen.

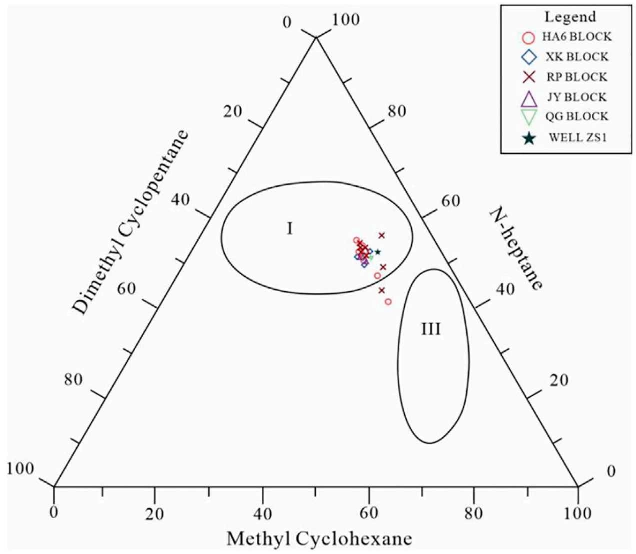


**FIGURE 5 |** Triangular plot of $C_7$ light hydrocarbon family composition of Halahatang Ordovician crude oil.

gammacerane in highly evolved Cambrian source rocks is due to the fact that gammacerane was fractured from kerogen early and preserved in the source rock inclusions. High content of gammacerane has been detected in many reservoirs of bitumen. Gammacerane was detected in only part of the crude oil, but not in some of the crude oil, which is due to the uneven mixing of the mature and highly mature oils generated in the late Cambrian with the previously accumulated oils. Gammacerane was detected in all the reservoir bitumen in well Zhongshen 1, and some of the oil produced in the same section contained gammacerane and some did not.

## 4.2 Geochemical Characteristics of Crude Oil

### 4.2.1 Components of Light Hydrocarbons

Light hydrocarbon is an important component of condensate and crude oil, and the content of light hydrocarbon accounts for about 1/4 to 1/3 of the total crude oil (Hunt et al., 1980; Wang et al., 1989), the content of light hydrocarbon is higher in condensate oil, while the content of biomarkers is only 1% or less in crude oil. In reflecting the overall characteristics of crude oil, the information from light hydrocarbon is more representative than that from biomarkers. The composition characteristics of light hydrocarbons are related to the type and maturity of kerogens (Thompson, 1979,1983; Wang et al., 1989; Wang and Coward, 1990; and 1994).

The $C_4$-$C_7$ light hydrocarbon family composition of the Halahatang Ordovician crude oil shows that the paraffin content is mainly 52.15–77.08%, the aromatic content is 0.18–1.68%, and the cycloalkane content is 22.46–46.32%, which means that the oil is relatively rich in paraffin and poor in aromatic hydrocarbons. This is typical of oil sourced from sapropelic source rocks (**Figure 4**). In addition, the arene content of halahatang Ordovician crude oil is very low, and benzene is not even detected, which is related to early water washing.

In the $C_7$ light hydrocarbon composition of crude oil, the contents of n-heptane, methylcyclohexane, and dimethyl cyclopentane are 40.76–55.84%, 30.99–44.02%, and 9.03–16.11%, respectively. The analysis results are put on the triangular plot of $C_7$ light hydrocarbon family composition (**Figure 5**), and almost all samples fall in the region of type I kerogen.

With the increase of maturity, the degree of alkylation of condensate of light hydrocarbon increases (Philip and Jolicoeur, 1975), while the degree of alkylation also increases (Thompson, 1979; Thompson, 1983). In order to quantify the maturity, two parameters, namely heptane value, and isoheptane value, are proposed to reflect the maturity. Heptane and isoheptane numbers were used to measure the degree of alkylation of light hydrocarbons in sediments. Thompson gave two lines, one aliphatic line representing the sapropelic kerogen and the other aromatic line representing the humic kerogen, and the region between the two lines should be the region of the mixed type, assuming that cycloalkanes open the ring to form alkanes.

The heptane value of halahatang Ordovician crude oil ranges from 29.02 to 40.74%, and the isoheptane value ranges from 1.45% to 3.06%. As can be seen from **Figure 6**, the sample data of Halahatang Ordovician crude oil falls above the aliphatic line, which again indicates that these condensate and crude oil are sapropelic kerogen sources. In addition, according to the maturity reflected by heptane and isoheptane values in **Figure 6**, the oil mainly belongs to the high maturity stage.

### 4.2.2 Medium Molecular Weight Hydrocarbon Characteristics of Crude Oil

The comparative study of medium molecular weight hydrocarbons is a new method for the comparative study

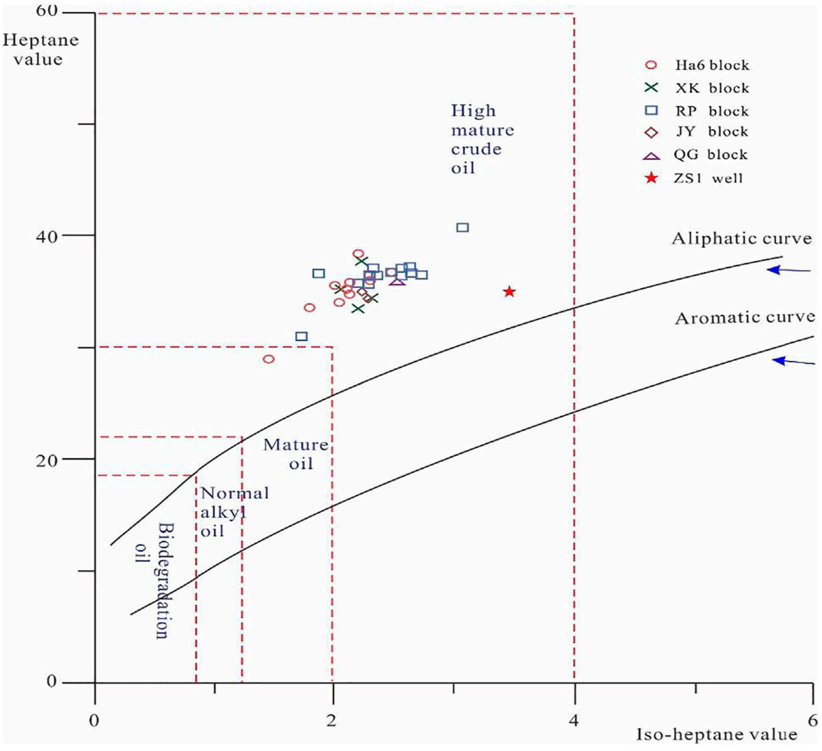


**FIGURE 6 |** The relationship between heptane and isoheptane values of Halahatang Ordovician crude oil.

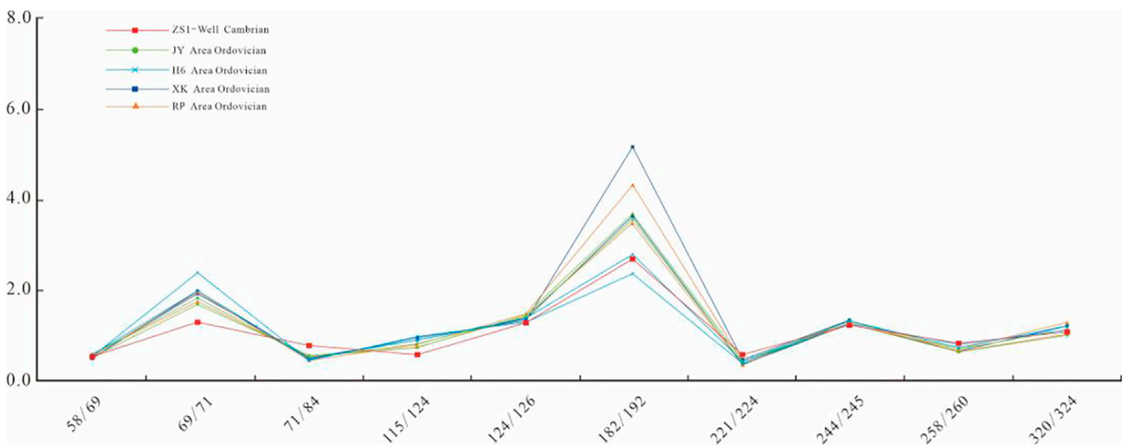


**FIGURE 7 |** Comparison of medium molecular weight hydrocarbons in the crude oil from well Zhongshen 1 to the Halahatang Area. Note (58: n-propylcyclohexane; 69: 2-methylnonane ($C_{10}$ isoalkane); 71: 3-methylnonane ($C_{10}$ transisoalkane); 84: 2,6 dimethyl Nonane ($C_{11}$ isoalkane); 115: n-pentylcyclohexane + 1-methyldecanes; 124: 2-methylundecane ($C_{12}$ isoalkane); 126: 3-methylundecane ($C_{12}$ transisoalkane); 150: 4-methyldodecane; 153: 3-methyldodecane ($C_{13}$ transisoalkane); 182: 2,6,10-trimethyldodecane; 192: Decane with $C_5$ as a substituent; 221 (n-decylcyclohexane + 7-methylpentadecane + 6-methylpentadecane); 224: 2-methylpentadecane ($C_{16}$ isoalkane); 258: n-undecylcyclohexane+5-methylheptadecane; 260: 2-methylheptadecane ($C_{18}$ isoalkane); 309: 2-methyleicosane ($C_{21}$ isoalkane); 311 : 2,6,10,14-tetramethylnonadecane).

of oils in recent years, which mainly uses compounds of similar molecular weight to form compound pairs (Hwang et al., 1994). Medium molecular weight compounds, which means having the same carbon number in general include isoalkane, transisoalkane, and a methyl substituent of other alkanes and isopentadiene alkanes, these compounds have a common characteristic, that is the life source of bacteria, but different types of bacteria influence on the distribution of these compounds is very strong, so it can be used for oil-oil comparison, and the content of this kind of compound is

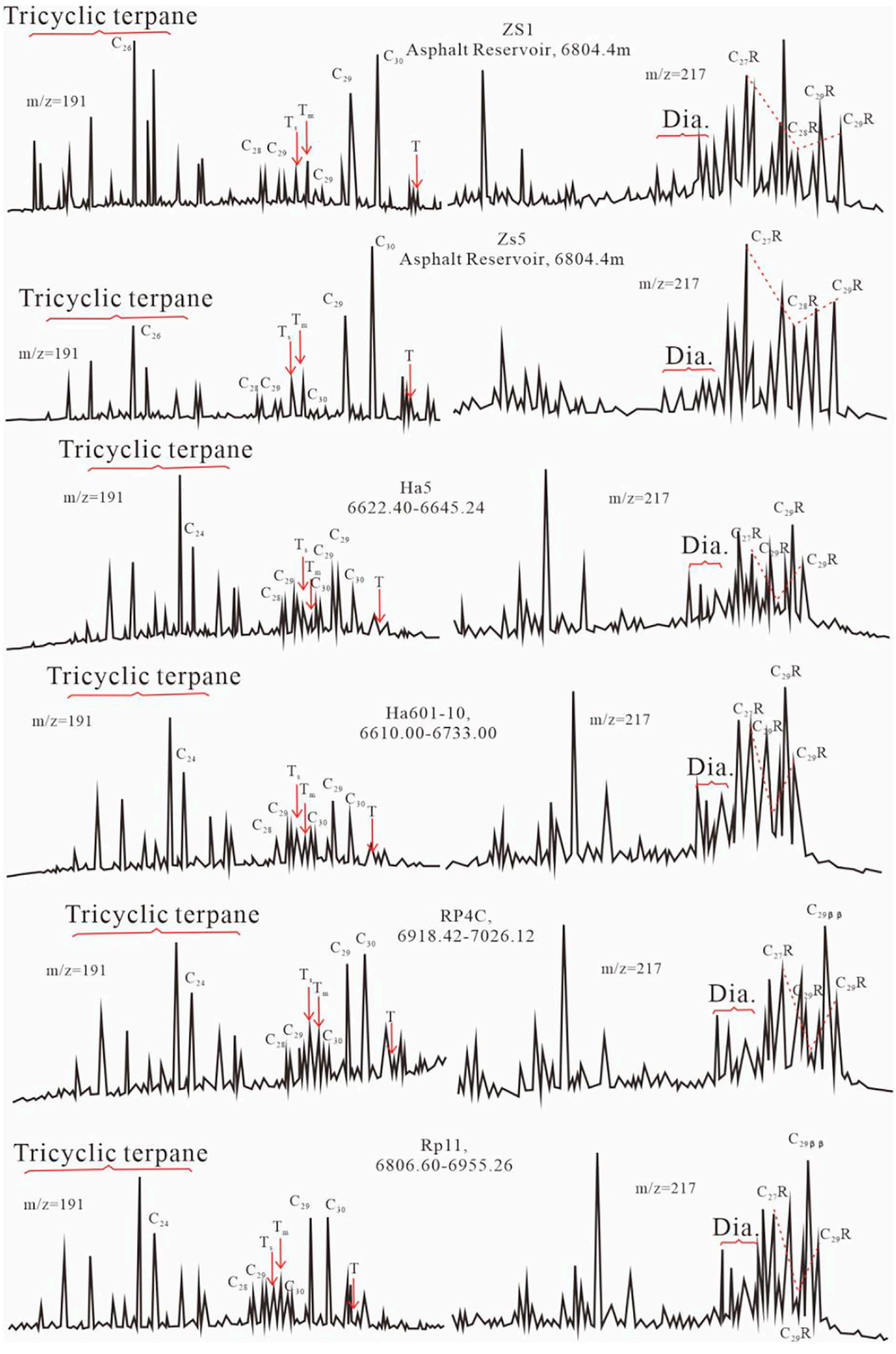


**FIGURE 8 |** Chromatograms of terpanes and steranes in Ordovician crude oils from Halahatang and its surrounding areas.

very high, with high-resolution chromatography can be identified, generally using all-oil chromatography. (Hwang et al., 1994).

The fingerprint comparison of medium molecular weight hydrocarbon of Cambrian oil from well Zhongshen 1 and crude oil from halahatang blocks shows that there are obvious

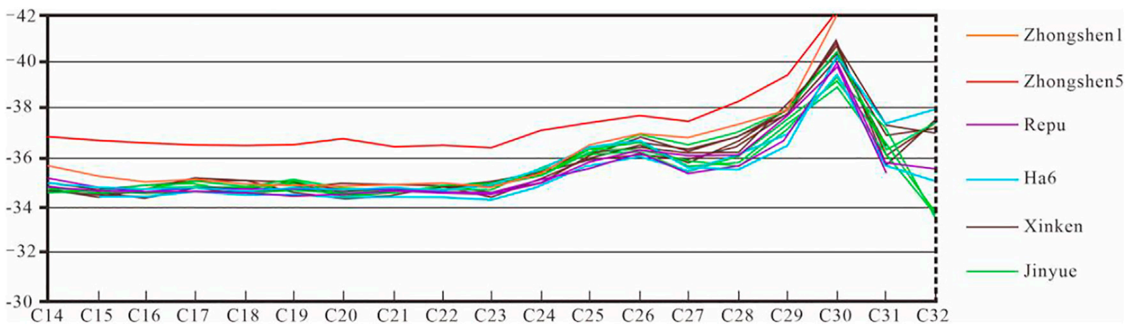


**FIGURE 9 |** Distribution of carbon isotopes of crude oil monomer hydrocarbon in the Halahatang Area.

**TABLE 2 |** Ordovician natural gas composition data table in the Halahatang Area (only some data are shown).

| Well no. | Horizon | Gas composion/% | | | | | | | | | $H_2S$ (ppm) | $C_1/C_1^+$ |
|---|---|---|---|---|---|---|---|---|---|---|---|---|
| | | $CH_4$ | $C_2H_6$ | $C_3H_8$ | $iC_4H_{10}$ | $nC_4H_{10}$ | $iC_5H_{12}$ | $nC_5H_{12}$ | $C_6H_{14}$ | $N_2$ | | |
| H6-1 | $O_2y$ | 66.80 | 14.90 | 6.82 | 1.20 | 2.15 | 0.54 | 0.54 | 0.36 | 4.6 | | 0.72 |
| H6C | O | 82.80 | 8.43 | 2.23 | 0.24 | 0.38 | 0.07 | 0.06 | 0.03 | 4.82 | | 0.88 |
| H7 | O | 53.20 | 15.80 | 8.57 | 1.13 | 3.05 | 0.87 | 0.69 | 0.53 | 5.01 | 8.90E+04 | 0.63 |
| H8 | O | 49.70 | 6.85 | 2.82 | 0.62 | 1.07 | 0.31 | 0.30 | 0.20 | 5.76 | | 0.80 |
| H9 | O | 58.50 | 16.30 | 4.35 | 0.37 | 0.83 | 0.10 | 0.10 | 0.03 | 3.79 | | 0.73 |
| H601 | O | 65.80 | 16.10 | 6.45 | 0.75 | 1.55 | 0.30 | 0.34 | 0.22 | 7.72 | | 0.72 |
| H602 | O | 83.50 | 7.18 | 3.96 | 0.94 | 1.52 | 0.43 | 0.38 | 0.26 | 1.01 | 5.20E+01 | 0.85 |
| H602-1 | $O_2y$ | 73.90 | 2.44 | 0.48 | 0.05 | 0.09 | 0.02 | 0.02 | 0.01 | 3.08 | | 0.96 |
| H603 | O | 36.60 | 7.33 | 4.19 | 0.89 | 1.87 | 0.61 | 0.67 | 0.48 | 2.01 | | 0.70 |
| XK4 | O | 66.90 | 16.60 | 2.49 | 0.59 | 0.90 | 0.24 | 0.21 | 0.12 | 5.28 | 1.40E+02 | 0.76 |
| XK4 | O | 57.90 | 14.20 | 10.50 | 2.42 | 3.63 | 0.89 | 0.78 | 0.45 | 4.55 | 3.10E+02 | 0.64 |
| XK5 | O | 67.60 | 11.50 | 6.08 | 1.39 | 2.13 | 0.60 | 0.55 | 0.38 | 4.09 | | 0.75 |
| XK6 | $O_1y$ | 78.40 | 7.07 | 4.21 | 1.07 | 1.58 | 0.56 | 0.47 | 0.30 | 2.85 | | 0.84 |
| XK601 | O | 59.80 | 4.18 | 1.03 | 0.06 | 0.14 | 0.03 | 0.02 | 0.03 | 6.15 | 1.13E+04 | 0.92 |
| RP11 | $O_2y$ | 78.10 | 7.95 | 4.33 | 0.92 | 1.40 | 0.35 | 0.31 | 0.22 | 4.75 | | 0.83 |
| RP12 | $O_2y$ | 81.80 | 3.82 | 0.91 | 0.10 | 0.17 | 0.04 | 0.04 | 0.05 | 7.35 | | 0.94 |
| RP13 | O | 63.40 | 9.76 | 5.95 | 1.56 | 2.35 | 0.78 | 0.64 | 0.58 | 3.16 | | 0.75 |
| RP14 | O | 63.00 | 10.10 | 8.90 | 2.65 | 4.42 | 1.46 | 1.31 | 1.08 | 4.57 | | 0.68 |
| RP2 | $O_2y$ | 70.40 | 12.80 | 6.89 | 1.27 | 1.82 | 0.44 | 0.39 | 0.34 | 4.95 | | 0.75 |
| RP3 | $O_2y$ | 83.60 | 6.63 | 2.79 | 0.65 | 0.81 | 0.21 | 0.15 | 0.09 | 3.67 | 7.3 | 0.88 |
| RP3001 | $O_2y$ | 83.30 | 6.13 | 2.96 | 0.73 | 0.99 | 0.26 | 0.20 | 0.13 | 3.91 | | 0.88 |
| RP8 | O | 71.70 | 10.70 | 6.09 | 1.33 | 1.87 | 0.44 | 0.32 | 0.14 | 5.84 | 0 | 0.77 |

similarities between Cambrian oil from well Zhongshen 1 and crude oil samples from Halahatang blocks (**Figure 7**).

### 4.2.3 Characteristics of Biomarker Compounds

The content of long -chain tricyclic terpenes in Ordovician crude oil from Halahatang is higher, usually higher than that of pentacyclic terpenes; the content of $C_{29}\beta\beta$ is generally higher, which is due to high maturity or long migration distance. The content of gammacerane in the Ordovician crude oil of Halahatang is generally not high. According to the latest research results, maturity also has a crucial influence on the content of gammacerane in crude oil, and the relative content of gammacerane will change in different thermal evolution stages.

High content of gammacerane was detected in the Ordovician reservoir bitumen in the Halahatang block. The content of long-chain tricyclic terpenes varies. $C_{27}R$, $C_{28}R$, and $C_{29}R$ steranes are in the shape of "V" distributed. In addition, a relatively high content of gammacerane was also detected in the reservoir bitumen of well Zhongshen 5 and Zhongshen 1, and the oil produced in the same well section contains gammacerane, while others do not contain gammacerane (**Figure 8**).

### 4.2.4 Carbon Isotope Characteristics of Crude Oil

Statistics show that the carbon isotope of organic matter has a chronological effect and generally becomes heavier as the geological age becomes newer. The kerogen carbon isotope of the Cambrian source rock in the Tarim Basin is heavier than the kerogen isotope of the Upper Ordovician source rock. The former is mainly distributed in −35.6~−29.5‰, and the latter is mainly distributed in −31.29~−29.69‰, which is mainly related to the evolution of biology. Cambrian source rocks and Ordovician source rocks are close in age. Although the carbon isotope age effect indicates that the carbon isotope of oil generated from Cambrian source rocks is lighter than that of oil generated from Ordovician source rocks, it is still difficult to define the specific value.

**TABLE 3 |** Carbon isotope analysis data of Ordovician natural gas in the Halahatang Area.

| Well no. | Horizon | Depth/m | Carbon isotope/(VPDB)‰ | | | |
|---|---|---|---|---|---|---|
| | | | $\delta CH_4$ | $\delta C_2H_6$ | $\delta C_3H_8$ | $\delta C_4H_{10}$ |
| H6 | C | 5,953–5,954 | −42.8 | −35.8 | −32.7 | −31.5 |
| H9 | O | 6,598.11–6,710 | −53 | −41.1 | −36.6 | −34.8 |
| H7 | O | 6,622.41–6,645.24 | −50.7 | −40 | −36 | −33.8 |
| H11 | O | 5,668–5,748 | −46.3 | −36.1 | −34.0 | −31.1 |
| H10 | O | 6,618.5–6,700.83 | −52.2 | −39.8 | −36.6 | −36.6 |
| H13 | O | 6,668.5–6,800 | −46.9 | −37.2 | −33.5 | −32.2 |
| H601 | O | 6,598.23–6,677 | −48.7 | −40.1 | −37.8 | −34.2 |
| H12 | O | 6,615.5–6,726 | −48.5 | −37.7 | −35.5 | −32.2 |
| H701 | O | 6,557.89–6,618 | −50.9 | -40.2 | −36.7 | −33.5 |
| H11-1 | O | 6,598–6,697 | −46 | −35.4 | −31.9 | −31 |
| H601-2 | O | 6,556.08–6,664.72 | −47.2 | −36.8 | −35.2 | −32 |
| H11-2 | O | 6,653.63–6,719.08 | −45.9 | −38.3 | −32.3 | −30.5 |
| H12-1 | O | 6,597.6–6,715 | −46 | −35.4 | −32.8 | −31.4 |
| H12-2 | O | 6,597.56–6,745 | −47.9 | −37.5 | −34.4 | −32.8 |
| H15 | O | 6,512.61–6,668 | −48.3 | −39.6 | −35.4 | −32.5 |
| H16 | O | 6,616–6,646 | −49.2 | −39.9 | −35.7 | −33.9 |
| H702 | O | 6,594–6,660 | −48.2 | −38.3 | −35.3 | −33.3 |
| H7-3 | O | 6,605–6,666 | −50.3 | −39.9 | −35.4 | −34.4 |
| H902 | O | 6,666–6,690 | −51.4 | −40.6 | −35.4 | −32.5 |
| XK4 | O | 6,834.05–6,850 | −47.5 | −37.7 | −33.8 | −31.4 |
| XK6 | O | 6,831–6,920 | −45.7 | −35.1 | −32.6 | −30.6 |
| XK7 | O | 6,880–6,980 | −46.3 | −35.6 | −32.7 | −30.8 |
| XK7C | O | 6,900–6,935 | −45.6 | −35.1 | −32 | −28.3 |
| XK9c | O | 6,757–7,011 | −46.8 | −37.7 | −32.4 | −30.4 |
| RP13 | O | 6,853–6,890 | −47.76 | −36.84 | −32.34 | −30.24 |
| RP3-1 | O | 6,966–7,066 | −47.28 | −34.4 | −25.90* | # |
| RP301 | O | 7,006–7,069 | −45.22 | −39.35 | −31.49 | −30.96 |
| RP6C | O | 6,534–7,220 | −46.83 | −37.05 | −34.24 | # |

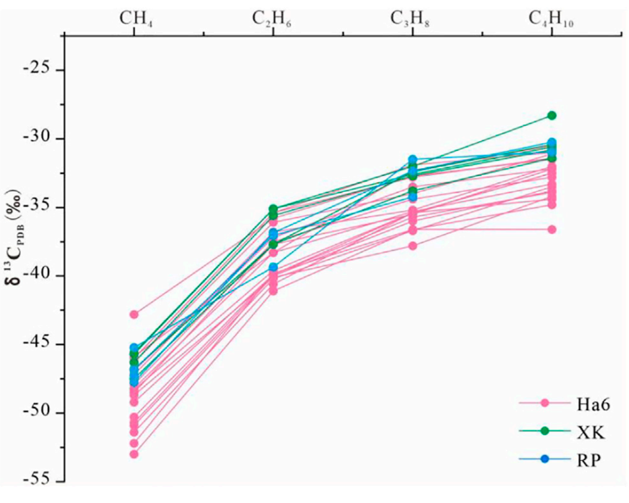


**FIGURE 10 |** Line chart of C $_1$-C $_4$ carbon isotope values of Ordovician natural gas in the Halahatang Area.

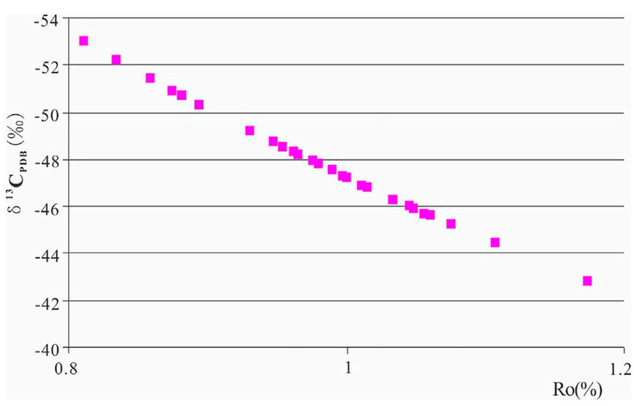


**FIGURE 11 |** δ $^{13}$C $_1$ -Ro relationship diagram of Ordovician natural gas in the Halahatang Area.

The carbon isotope of Halahatang crude oil is mainly distributed in −33.8~−32‰, and the carbon isotope of monomer hydrocarbon is basically consistent with the distribution curve of single hydrocarbon carbon isotope of crude oil of the Cambrian in wells Zhongshen 1 and Zhongshen 5 (**Figure 9**), indicating that they have the same source.

## 4.3 Natural Gas Geochemical Characteristics

### 4.3.1 Characteristics of Natural Gas Components

Through statistical analysis of the drying coefficients of 181 natural gas samples (including 116 samples in the Ha6 block, 27 samples in the Xinken block, and 38 samples in the Repu block) from the three main oil-producing areas in the Halahatang area: The drying coefficient of Ordovician natural gas in Lahatang

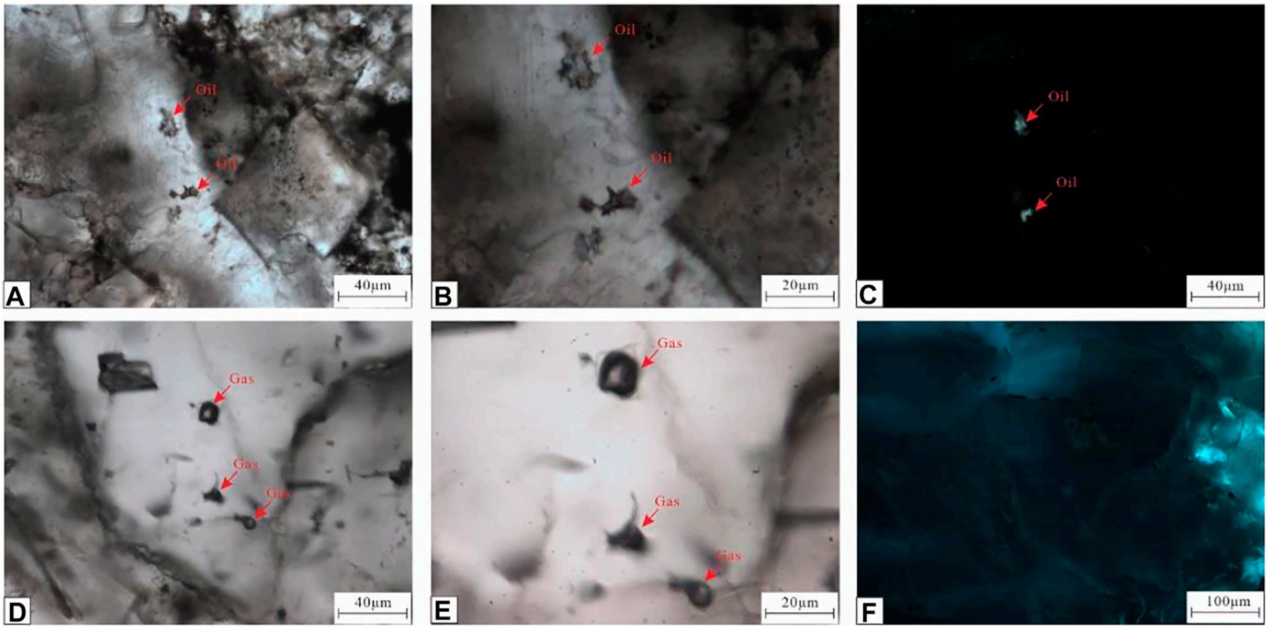


**FIGURE 12 |** Characteristics of fluid inclusions in Ordovician carbonate reservoirs in Repu block. **(A–C)** are liquid inclusions, **(D–F)** are gas phase inclusions **(A–C)** are liquid inclusions, DEF are gas phase inclusions.

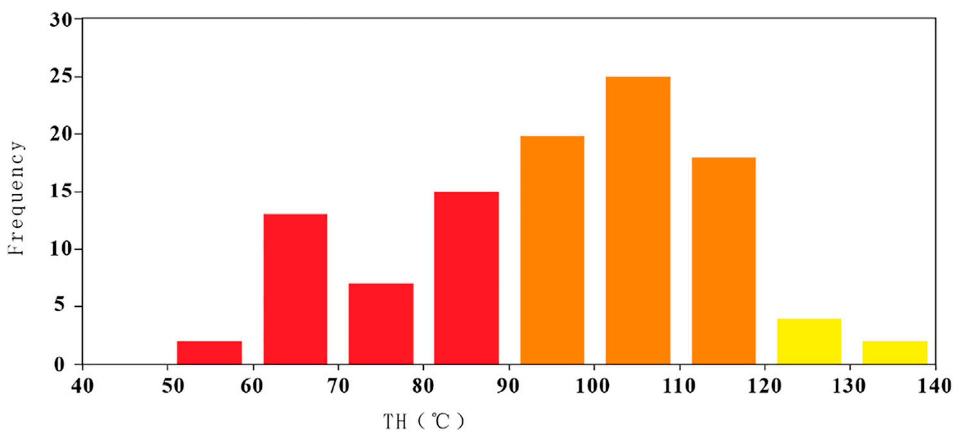


**FIGURE 13 |** Characteristics of fluid inclusions in Ordovician carbonate reservoirs in the Repu block.

area is relatively low. The drying coefficient of Ha 6 block is mainly distributed in the range of 0.7–0.8, and the drying coefficient of natural gas in Xinken and Repu blocks is mainly distributed between 0.75–0.85. Therefore, it is believed that the maturity of crude oil-associated gas in the north may be slightly lower than that in the south (**Table 2**).

The Ordovician natural gas in the Halahatang area is mainly associated with gas of crude oil, including hydrocarbon gas and non-hydrocarbon gas, among which methane, ethane, and propane are the main components of hydrocarbon gas, and the methane content is mainly between 30%–85% (12.7%–85.9%), the ethane content is mainly between 4%–16% (1.35%–20.5%), and the propane content is mainly between 1%–10% (0.01%–11.6%), and the drying coefficient is between 0.52 and 0.96. Through the further statistical division of the drying coefficient results of different oil-producing areas in the Halahatang area, the drying coefficient of the Ha 6 block is mainly between 0.7 and 0.8, and the drying coefficient of natural gas in the Xinken and Repu blocks is mainly between 0.75–0.85, which can be seen that the drying coefficient of natural gas in the south is slightly higher than that in the north. Nitrogen and hydrogen sulfide are the main components of non-hydrocarbon gases, and

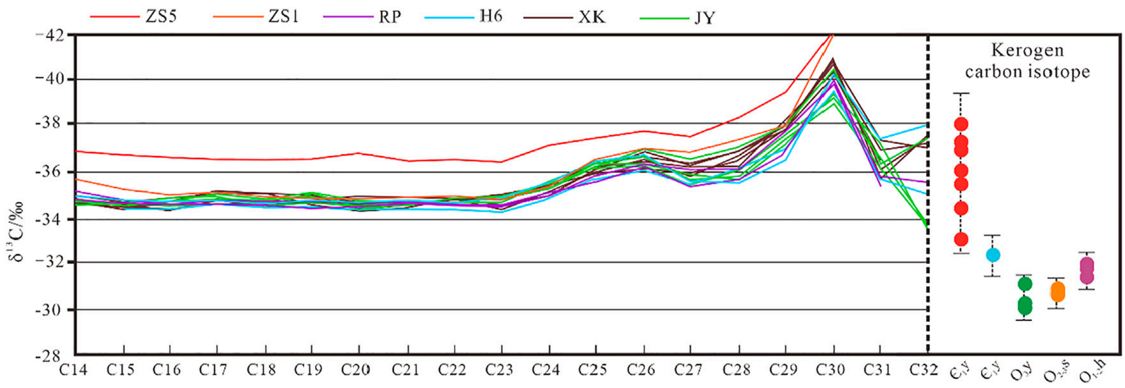


**FIGURE 14 |** Comparison of carbon isotope of crude oil monomer hydrocarbon and kerogen in the Halahatang Area.

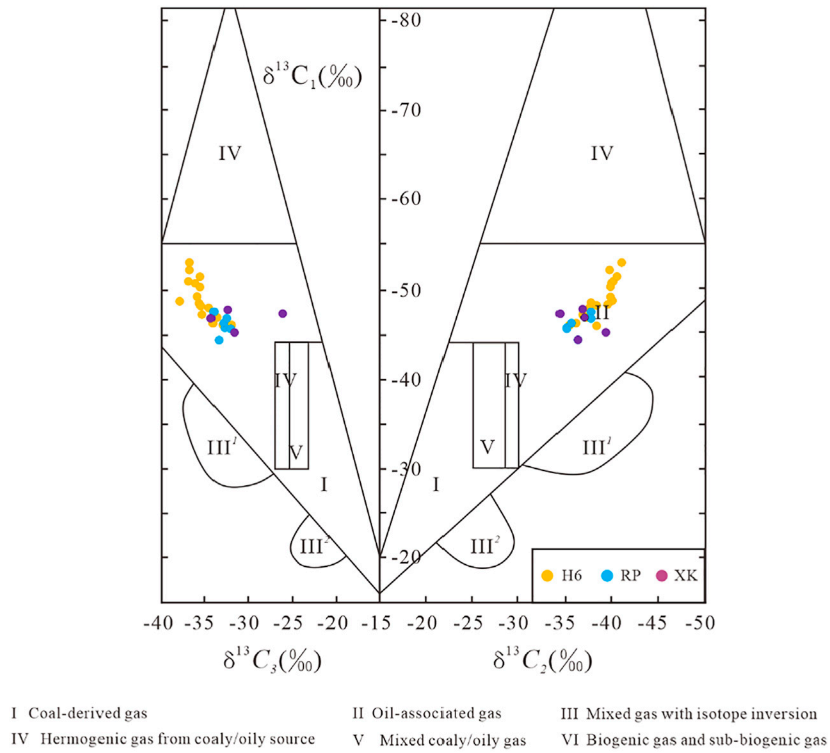


**FIGURE 15 |** Distribution characteristics of δ13C1-δ13C2-δ13C3 of Ordovician natural gas in the Halahatang Area.

the nitrogen content is relatively balanced, mainly between 3% and 5%. The nitrogen content of some wells in the southern part of the whole block is slightly higher than that in the northern part. The high hydrogen sulfide wells in the whole block are distributed in the heavy oil area, mainly in the well Ha 15 area, well Ha 7 area, and some wells in the well Ha 9 area.

The nitrogen content of the Ordovician natural gas in the Halahatang area is relatively balanced, generally between 3% and 5%, and the nitrogen content in the wells in the south of the entire block is slightly higher than that in the north. The high hydrogen sulfide wells in the whole block are distributed in the heavy oil area, mainly in the well Ha 15 area, the well Ha 7 area, and some wells in the well Ha 9 area. The reason for its high hydrogen sulfide may be related to the adsorption and desorption of hydrogen sulfide by colloidal or asphaltenes. The natural gas produced in the southern block is essentially free of hydrogen sulfide.

### 4.3.2 Carbon Isotope Characteristics

Previous studies have shown that the $\delta^{13}C_2$ of natural gas from humic sources is higher than −25.1‰, while the $\delta^{13}C_2$ of natural gas from sapropelic sources is lower than −28.8‰ (Dai, 1992).

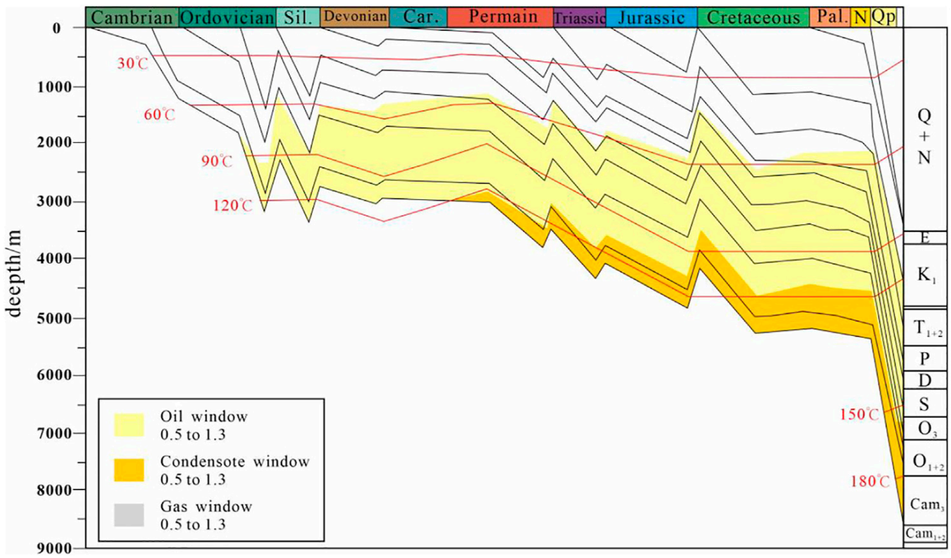


**FIGURE 16 |** Burial thermal evolution history of well Repu 4.

The overall distribution trend of $C_1$~$C_4$ carbon isotope content of natural gas in the Halahatang area is generally consistent, and the carbon isotope values are relatively light. The methane carbon isotope values of Ordovician natural gas in Halahatang are mainly distributed between −45.22‰ and −53‰, with an average of −47.7‰; The carbon isotope values of ethane are distributed between −41.1‰ and −34.4‰, with an average of −37.7‰; the carbon isotope values of propane are mainly distributed in the range of −31.49‰ to −37.8‰, with an average of 34.2‰; The carbon isotope values of butane are mainly distributed from −28.3‰ to −34.8‰, with an average of 32.2‰ (**Table 3**; **Figure 10**).

According to a large number of statistical data, Zhao et al. (2021) concluded that the methane carbon isotope values of associated gas in the reservoir were between −55‰ and −44‰, while Dai (1992) believed that the methane carbon isotope values of associated gas in the reservoir were between −55‰ and −40.4‰. But no matter which standard is used, the methane carbon isotope values of the Ordovician natural gas in the Halahatang area reflect that the natural gas in this area should belong to the associated gas of the oil reservoir (**Figure 11**). According to the formula of $\delta^{13}$C1-Ro ($\delta^{13}C_1$ = 27.550lgRo-47.22) (Zhao et al., 2021).

## 4.4 Characteristics of Fluid Inclusions

Fluid inclusions record the relevant information on oil and gas migration and accumulation and are of great significance to the analysis and study of accumulation stages. The formation of oil and gas inclusions represents the stage of oil and gas migration and charging. The homogeneous temperature of the inclusions records the paleo-geotemperature of the oil and gas migration and charging reservoirs. The burial depth of the inclusions can be determined through the restoration of thermal history and reservoir burial history, and the corresponding stratigraphic age is the age of hydrocarbon accumulation. The oil and gas components in the inclusions can reflect the geochemical characteristics and phase states of oil and gas (Wang et al., 2006, 2018).

Through the research on the fluid inclusions in the Ordovician reservoirs in the Repu structure in the Halahatang area, it is found that there are three formation processes in the homogenization temperature of the reservoir inclusions. The homogenization temperature of the inclusions in the first stage is from 70 to 90°C, and most of the inclusions are filled with liquid phase. In the second stage, the homogenization temperature of the inclusions is between 90 and 115°C, and most of the inclusions are characterized by a gas-liquid two-phase. In the third stage, the homogenization temperature of the inclusions is from 115 to 140°C, and the inclusions are mainly in the gas phase (**Figures 12**, **13**).

# 5 DISCUSSION

## 5.1 Oil and Gas Source Analysis

### 5.1.1 Oil Source Comparison

Some experts and scholars (Zhang et al., 2004; Zhang et al., 2000, 2002a, b, 2005; Hanson et al., 2000; Li et al., 2010a; Jiang et al., 2007) believe that the important source of current movable oil in the basin is the Middle-Upper Ordovician source rocks, and it is believed that the Cambrian-Lower Ordovician source rocks are not distributed in the Halahatang area, and the carbonate oil and gas in the Halahatang area mainly come from the Middle-Upper Ordovician source rocks. By analyzing the light hydrocarbons of the Ordovician crude oil in the study area, it is found that the Ordovician crude oil in the Halahatang area belongs to the highly mature oil, and the organic matter types of source rocks are type I and type II. The relative composition of $C_5$-$C_7$ light hydrocarbon

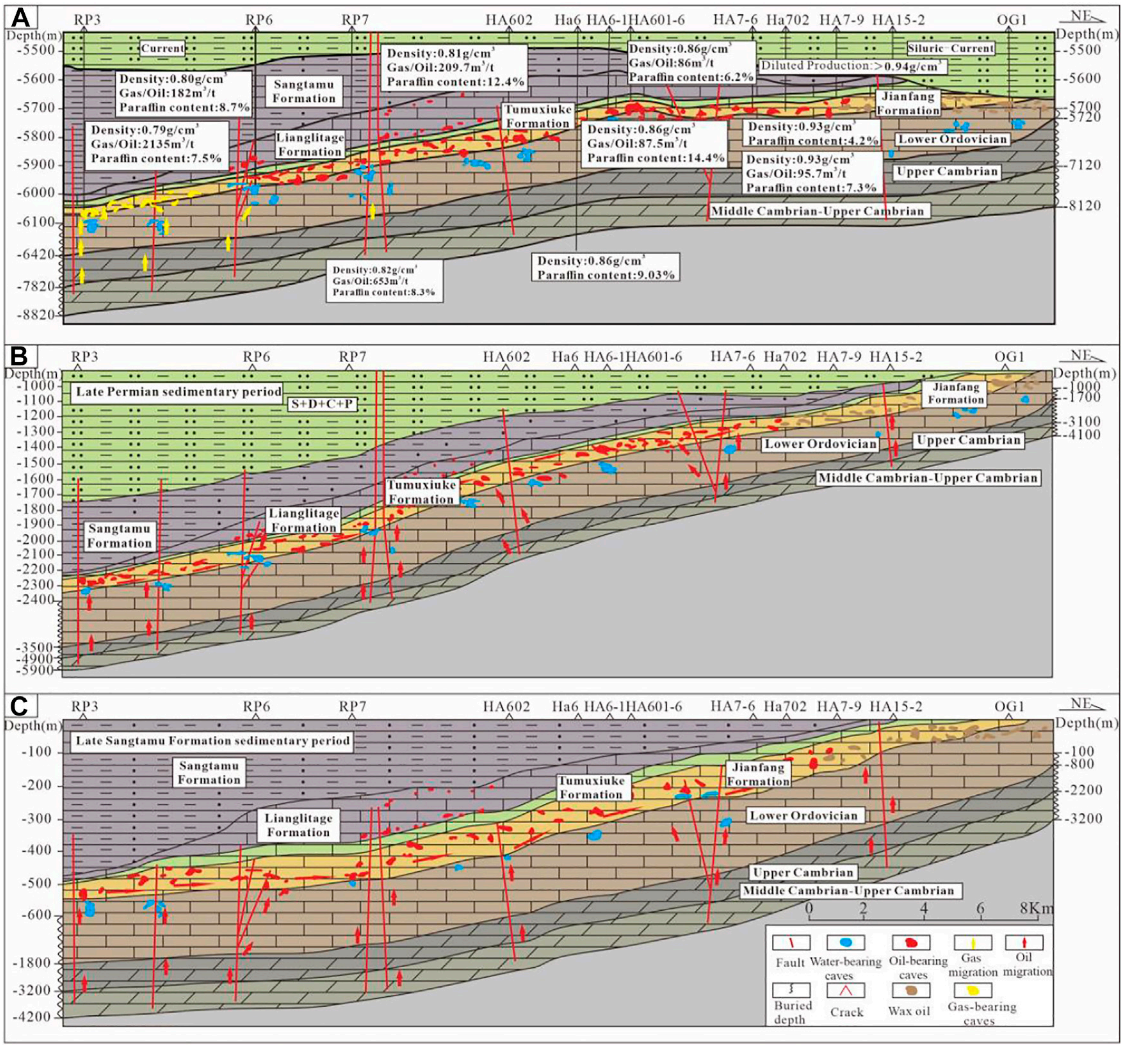


**FIGURE 17 |** Hydrocarbon accumulation model of Ordovician in the Halahatang Area, and Tarim Basin.

fractions of crude oil samples is dominated by n-paraffins, the relative composition of $C_7$ light hydrocarbon compounds is dominated by isoparaffins, and the crude oil source rocks are dominated by sapropelic organic matter.

The characteristics of molecular weight hydrocarbons and biomarker compounds in the Ordovician crude oil in the study area were analyzed and compared with the Cambrian crude oil in the well Zhongshen 1 area and the well Zhongshen 5 area. The results show that well Zhongshen 1 and well Zhongshen 5 are very similar to the Ordovician crude oil in the Halahatang area. Combined with the comparative study of carbon isotope of single hydrocarbon of crude oil and kerogen carbon isotope of Cambrian-Ordovician source rocks around the study area, it is considered that Ordovician crude oil in the study area is mainly derived from Cambrian source rocks. (**Figure 14**).

### 5.1.2 Comparison of Gas Sources

The above analysis shows that the kerogen type of the Cambrian-Lower Ordovician source rock is better than that of the Middle-Upper Ordovician source rock, and the Middle-Upper Ordovician source rock belongs to the marine sapropelic type source rock, which is biased to the humic type (Zhao et al., 1998). The carbon isotope of the natural gas is heavier than that of the natural gas from the typical marine sapropelic kerogen, although it does not fully reflect the characteristics of the natural gas from the terrestrial humic kerogen. Especially in natural gas, ethane isotopes should have an obvious reflection, that is, ethane carbon isotope is obviously heavy. Through the carbon isotope analysis of the Ordovician natural gas in the Halahatang area, it can be seen that the isotopes of methane and ethane are obviously lighter, and there is no characteristic of the source of humic kerogen. Therefore, it is inferred that the Ordovician natural gas in the study area is the crude oil-associated gas originating from the Cambrian (**Figure 15**).

The analysis found that the $N_2$ content in the Ordovician natural gas in the Halahatang area has the distribution characteristics of "high in the south and low in the north", indicating that there are differences in the migration paths and modes of oil and gas, and it is believed that oil and gas have two-way charging vertically and horizontally. Vertically, it was mainly the in-place Cambrian carbonate source rock that migrated upward through faults; horizontally, it was mainly the migration of oil and gas generated by the Cambrian mudstone source rock in the southern Manjiaer sag.

## 5.2 Time and Stage of Hydrocarbon Accumulation

Based on the study of the homogenized temperature of fluid inclusions in the reservoir and combined with previous studies (Zhang et al., 2013; Ding et al., 2020), it is believed that the accumulation stages of the Ordovician carbonate reservoirs in Halahatang are mainly three stages, which are Late Caledonian-Early Hercynian, Late Hercynian and Himalayan (**Figure 16**). The homogenization temperature of the first stage inclusions is 70–90°C, and most of the inclusions are filled with liquid phase. During this period, after the deposition of the Sangtamu Formation, the structural high part of the Halahatang sag was uplifted accordingly, and the strata in some areas may have suffered denudation and local biodegradation, resulting in the precipitation of asphalt in the reservoir. In the second stage, the homogenization temperature of inclusions is between 90 and 115°C, and most of the inclusions are characterized by a gas-liquid two-phase. The analysis shows that the oil and gas accumulation period is late Hercynian, which is the accumulation and supplement of early oil and gas along faults and structural fractures. In the third stage, the homogenization temperature of the inclusions is 115–140°C, and the inclusions are mainly gas phase. According to the analysis, the hydrocarbon accumulation period is the Himalayan period. The charging of the Ordovician reservoirs in the Repu area with the Cambrian or Middle-Upper Ordovician oil cracking gas, and the reformation of the original oil reservoirs, formed oil reservoirs with gas caps and some gas-invading condensate gas reservoirs.

## 5.3 Accumulation Model

According to the burial thermal evolution history of Well Repu 4 in the study area (**Figure 16**), the Cambrian source rocks reached the threshold of hydrocarbon generation during the Late Caledonian and Early Hercynian periods. With the increase of thermal evolution, the Ro of Cambrian source rocks in the late Hercynian reached above 0.7% and began to generate large amounts of oil. However, due to the relatively weak cap rock conditions at this time, the massive crude oil generally suffered serious biodegradation (**Figure 17**). A large amount of biodegraded bitumen can be found in the Ha 6 block, especially in the dissolution pores and cavities of the Ordovician reservoir in the northern buried hill zone and in the fractures not filled with calcite. High abundance of 25-norhopane was detected in crude oil samples from the Ha 6 block and most of the wells in the northern part of the Xinken block.

During the middle-late Caledonian period, the oil generated in the Cambrian system in the study area and the Cambrian system in the southern Manjiaer sag migrated and accumulated along the faults and transport layers from the south flank slope of Halahatang to the structural in the north. At the same time, the northern caprock may be denuded to varying degrees, and the crude oil will suffer from biodegradation to form bitumen precipitation. In the late Hercynian period, oil and gas migrated from the south to the north again along faults and transport layers. However, due to the plugging of the reservoir pores by the bitumen produced by the biodegradation of the oil and gas-charged in the early stage, the fracture fractures and the physical properties of the reservoir in the study area are different to varying degrees, and the oil and gas generated from the Cambrian source rocks in the southern Manjiaer sag are filled in some pores or fractures that are not blocked by bitumen. Therefore, the migration and accumulation to the northern structural high were restricted, and the hydrocarbons generated in the Cambrian *in situ* during this period continued to migrate and accumulate vertically to the Ordovician reservoir along the oil source fault. During the Himalayan period, the natural gas generated in the in-place Cambrian continued to migrate vertically along the fault in-place. Due to the early blocking of asphalt in the high part of the structure in the north, only a small amount of condensate gas formed in the later period was charged or almost failed to affect the gas invasion of the reservoir. Therefore, Ordovician reservoirs in some wells maintain the wet gas characteristics of crude oil-associated gas, and most of them form oil and gas reservoirs with gas caps. While the natural gas migration and accumulation of well Repu 3 located near the lower part of the south wing slope structure are large, the paleo-reservoir was transformed by gas invasion, forming a secondary high-wax oil reservoir with a high gas-oil ratio greater than 2000 $m^3$/t, and forming condensate gas reservoir.

# 6 CONCLUSION

1) The Ordovician crude oil in the Halahatang area is shown to be a typical source of kerogen in sapropelic source rocks. It belongs to the oil produced in the mature to high maturity stage, and the fingerprint characteristics of medium molecular weight hydrocarbons have good comparability with the crude oil in the Halahatang area. The crude oil biomarker compounds all showed high content of long-chain tricyclic terpenes and high Ts/Tm values, reflecting the characteristics of high-mature oil, and had a good corresponding relationship with the Cambrian source rock terpane map. At the same time, because a small amount of oil from the late Middle and Upper Ordovician was mixed into the crude oil of most wells, it showed the characteristics of low gammacerane content and a large rearranged sterane/regular sterane ratio. Comprehensive analysis shows that the oil and gas in the

Halahatang area mainly comes from the Cambrian source rocks.

2) Although the Ordovician natural gas in the Halahatang area is mainly composed of methane, the methane content in the crude oil-associated gas in most wells is only about 60%, and the drying coefficient is between 0.7 and 0.85, showing a trend of high in the south and low in the north. Judging from the plane distribution of nitrogen content in the study area, which is low in the south and high in the north, it is concluded that there is a vertical and horizontal bidirectional hydrocarbon migration and charging mechanism in the study area. The vertical direction is mainly the migration of oil and gas generated by the Cambrian carbonate rocks accumulated *in situ*, while the lateral direction is mainly the migration of oil and gas generated by the Cambrian mudstone source rocks in the southern Manjiaer sag. Through the study of natural gas carbon isotopes, it is concluded that the gas source rocks of natural gas in the Halahatang area are mainly sapropelic source rocks, which belong to the associated gas of oil reservoirs.
3) There are three stages of accumulation in the Ordovician in the Halahatang area: The Cambrian reached the hydrocarbon generation threshold in the middle and late Caledonian periods, while the Cambrian source rocks located in the Manjiaer sag in the south of Halahatang and the deep layers of the in-place entered a large amount of oil-generating stage, and the oil at the mature stage entered the Ordovician reservoir in the Repu area, forming the Ordovician oil reservoir. The late Hercynian period is the secondary replenishment and charging period of the reservoir, and some condensate oil and gas are generated at the same time. During the Himalayan period, a large amount of condensate gas generated in the Cambrian migrated upward along the faults and carried out gas-invasion reformation on the overlying strata, forming oil and gas reservoirs with gas caps and gas-intrusion-type condensate gas reservoirs.

## DATA AVAILABILITY STATEMENT

The original contributions presented in the study are included in the article/Supplementary Material, further inquiries can be directed to the corresponding authors.

## AUTHOR CONTRIBUTIONS

FH: Methodology, Software, Investigation, Writing Original Draft. XW: Validation, Formal analysis, Visualization. LL: Editing, Supervision, Data Curation. XL: Editing, Supervision, Data Curation. XY: Conceptualization, Reviewing and Editing. CS: Resources, Data Curation. LL: Editing, Data Curation. YR: Editing, Data Curation. HH: Editing, Supervision, Data Curation. All authors have read and agreed to the published version of the manuscript.

## FUNDING

This research was funded by Key Laboratory of Sedimentary Basins and Petroleum Resources, Ministry of Natural Resources of China (No. cdcgs2020004), China Postdoctoral Science Foundation (2021M690485).

## ACKNOWLEDGMENTS

The authors would like to thank all the reviewers and editors for the constructive help in manuscript revision.

## REFERENCES

Anlai, M. H., Li, J. H., Li, X. P., Gao, X., Wang, F., and Yao, Y. (2020). Geochemical Characteristics of Middle-Upper Ordovician Source Rocks in the Kalpin Outcrop Profiles and Marine Oil-Source Correlation, Tarim Basin, NW China. *J. Nat. Gas Geoscience* 5 (3), 143–155. doi:10.1016/j.jnggs.2020.04.001

Chang, X. C., Wang, T. G., Tao, X. W., and Zhang, F. (2015). Aromatic Biomarkers and Oil Source of the Ordovician Crude Oil in the Halahatang Sag, Tarim Basin. *Oil Gas Geol.* 36 (02), 175–182. doi:10.1080/10916466.2018.1558242

Chen, H. H., Wu, Y., Feng, Y., Ziye, L., Shouzhi, H., and Lu, Y. (2014). Timing and Chronology of Hydrocarbon Charging in the Ordovician of Tahe Oilfield, Tarim Basin, NW China. *Oil Gas Geol.* 35 (06), 806–819. doi:10.11743/ogg20140608

Cheng, B., Wang, T. G., and Chang, X. C. (2013). Application of C5-C7 Light Hydrocarbons in Geochemical Studies:A Case Study of Ordovician Crude Oils from the Halahatang Depression, Tabei Uplift. *Nat. Gas. Geosci.* 24 (02), 398–405.

Dai, J. X. (1992). Identification of Various Alkane Gases. *Sci. Sin.* (02), 185–193.

Ding, Z., Wang, R., Chen, F., Yang, J., Zhu, Z., and Yang, Z. (2020). Origin, Hydrocarbon Accumulation and Oil-Gas Enrichment of Fault-Karst Carbonate Reservoirs: A Case Study of Ordovician Carbonate Reservoirs in South Tahe Area of Halahatang Oilfield, Tarim Basin. *Petroleum Explor. Dev.* 47 (2), 306–317. doi:10.1016/S1876-3804(20)60048-9

Hanson, A. D., Zhang, S. C., Moldowan, J. M., Liang, D. G., and Zhang, B. M. (2000). Molecular Organic Geochemistry of the Tarim Basin, Northwest China. *AAPG Bull.* 84 (8), 1109–1128. doi:10.1306/a9673c52-1738-11d7-8645000102c1865d

He, D. Y., Li, F. S., Hu, J. J., and Cuil, L. (2022). Geochemical Characteristics of H2S-Bearing Natural Gas from Halahatang Sag. *J. China Univ. Petroleum(Edition Nat. Sci.* 46 (01), 44–52. doi:10.1260/0144-5987.32.4.691

Hunt, J. M., Huc, A. Y., and Whelan, J. K. (1980). Generation of Light Hydrocarbons in Sedimentary Rocks. *Nature* 288 (5792), 688–690. doi:10.1038/288688a0

Hwang, R. J., Ahmed, A., and Moldowan, J. M. (1994). Oil Compostion Variation and Reservoir Continuity: Unity Field, Sudan. *Org. Gecchemistry* 21 (2), 171–188.doi:10.1016/0146-6380(94)90153-8

Jiang, N. H., Zhu, G. Y., Zhang, S. C., and Wang, Z. J. (2007). Detection Of2-Thiaadamantanes in the Oil from Well TZ-83in Tarim Basin and Itsgeological Implication. *Chin. Sci. Bull.* 52 (24), 2871–2875. (in Chinese). doi:10.1007/s11434-007-0407-6

Li, F., Zhu, G. Y., and Lv, X. X. (2021). The Disputes on the Source of Paleozoic Marine Oil and Gas and the Determination of the Cambrian System as the Main Source Rocks in Tarim Basin. *Acta Pet. Sin.* 42 (11), 1417–1436. doi:10.1016/j.jnggs.2016.05.002

Li, S., Amrani, A., Pang, X., Yang, H., Said-Ahmad, W., Zhang, B., et al. (2015). Origin and Quantitative Source Assessment of Deep Oils in the Tazhong Uplift, Tarim Basin. *Org. Geochem.* 78, 1–22. doi:10.1016/j.orggeochem.2014.10.004

Li, S. M., Pang, X. Q., Jin, Z. J., Yang, H. J., Xiao, Z. X., Gu, Q. Y., et al. (2010a). Petroleum Source in the Tazhong Uplift, Tarim Basin: New Insights from Geochemical and Fluid Inclusion Data. *Organic* 41 (6), 531–553. doi:10.1016/j.orggeochem.2010.02.018

Li, S. M., Pang, X. Q., Zhang, B. S., Xiao, Z. Y., and Gu, Q. (2010b). Oil-source Rock Correlation and Quantitative Assessment of Ordovician Mixed Oils in the Tazhong Uplift, Tarim Basin. *Petroleum Sci.* 7 (2), 179–191. doi:10.1007/s12182-010-0025-9

Li, Z., Huang, S. J., Liu, J. Q., and Pang, X. (2010). Buried Diagenesis, Structurally Controled Thermal-Fuid Process and Their Effect on Ordovician Carbonate Resercoir in Tahe, Tarim Basin. *Acta Sedimentol. Sin.* 28 (5), 969–979. (in Chinese with English abstract). doi:10.1016/j.marpetgeo.2013.03.002

Ni, X. F., Zhang, L. J., and Shen, A. J. (2009). Paleokarstificationtypes Karstification Periods and Superimposition Relationship of Ordo-Vician Carbonates in Northern Tarim Basin. *Geol. China* 36 (6), 1312–1321.

Philip, P. R., and Jolicoeur, C. (1975). The Scaled-Particle Theory and Solvent Isotope Effects on the Thermodynamic Properties of Inert Solutes in Water and Methanol. *J. Solut. Chem.* 4 (2), 105–125. doi:10.1007/bf00649153

Shen, A. J., Wang, Z. M., Zheng, X. P., He, X., and Zheng, D. (2007). Genesis Classification and Characteristics of Cambrian-Ordovician Carbonate Reservoirs and Petroleum Exploration Potential in Yaka-Yengimahalla area,Tarim Basin. *Mar. Orig. Pet. Geol.* 12 (2), 2332. (In Chinese).

Thompson, K. F. M. (1983). Classification and Thermal History of Petroleum Based on Light hydrocarbonS. *Geochimica Cosmochimica Acta* 47 (2), 303–316. doi:10.1016/0016-7037(83)90143-6

Thompson, K. F. M. (1979). Light Hydrocarbons in Subsurface Sediments. *Geochimica Cosmochimica Acta* 43 (5), 657–672. doi:10.1016/0016-7037(79)90251-5

Wang, F. Y., Feng, W. P., Guan, J., and Choa, J. (2018). Key Questions of the Fluid Inclusion Analysis in Petroliferous Basins and Their Significances. *Acta Metallurgica Sinica* 37 (3), 441–450. doi:10.19658/j.issn.1007-2802.2018.37.092

Wang, F. Y., Shi, Y. L., Zeng, H. S., and Liu, K. Y. (2006). To Identify Paleo-Oil Reservoir and to Constrain Petroleum Charging Model Using the Abundance of Oil Inclusions. *Bull. Mineralogy, Petrology Geochem.* 1, 12–18.

Wang, H. J., Zheng, G. K., and Chen, M. A. (1994). Excess Volumes of (Acrylonitrile Plus an Aromatic Hydrocarbon) at the Temperature 298.15-k. *J. Chem. Thermodyn.* 26 (5), 457–460. doi:10.1006/jcht.1994.1055

Wang, J., Doubleday, C., and Turro, N. J. (1989). Large Magnetic Field Effect on the Decay Rates of Triplet Hydrocarbon Diradicals. *J. Phys. Chem.* 93 (12), 4780–4782. doi:10.1021/j100349a019

Wang, Q., and Coward, M. P. (1990). The Chaidam Basin (NW China): Formation and Hydrocarbon Potential. *J. Ptroleum Geol.* 13 (1), 93–112. doi:10.1306/bf9ab6c2-0eb6-11d7-8643000102c1865d

Wu, Z. P., Chen, Z. H., Cao, Z. C., Liu, H., Cheng, B., and Chai, Z. (2020). Molecular Marker and Carbon Isotope Geochemistry of Ordovician Oils in the Tuofutai Bulge, Northern Tarim Basin: Implications for Oil Maturity, Source Characteristics and FIlling Directions. *Mar. Petroleum Geol.* 122, 104718. doi:10.1016/j.marpetgeo.2020.104718

Yan, L. L., Liu, Q. W., and Zhang, L. J. (2015). Diagenetic Environment for Ordovician Carbonate Rocks in Ha 6-Xinken Block of Halahatang Oilfield in Tarim Basin,China. *J. Chengdu Univ. Technol. Sci. Technol. Ed.* 42 (3), 288–295. doi:10.3969/j.issn.1671-9727.2015.03.04

Zhang, L. J., Fan, Q. H., and Zhu, Y. F. (2012). Geological and Accumulations Characteristics of Ordovician Oil Reser-Voir in Ha 6 Block of Tabei. *Petroleum Geology*. 2(2):7–12.

Zhang, N., Wang, Z. M., Ju, F. P., Xiao, Z., and Fang, Q. (2013). Diagenetic Bitumen in Ordovician Carbonate Reservoirs of the Northern Tarim Basin. *Acta Pet. Sin.* 34 (02), 225–231.

Zhang, Q. Y., Liang, B., and Cao, J. W. (2014). Palaeogeomorphologyand Karst Development Conditions of Yijianfang Formation in Hanilca-Tam Area. Fault-Block. *Oil & Gas. Field* 21 (4), 413–415. doi:10.1016/j.jngse.2014.10.028

Zhang, S. C., Liang, D. G., Li, M. W., Xiao, Z. Y., and He, Z. H. (2002a). Molecular Fossils and Oil Source Rock Correlations in the Tarim Basin, NW China. *Chinese Science Bulletin* 47, 20–27. doi:10.1007/bf02902814

Zhang, S. C., Liang, D. G., Zhang, B. M., Wang, F. Y., and Bian, L. Z. (2004). *Generation of Marine Oil and Gas in Tarim Basin*. Beijing: PetroleumIndustry Press. (in Chinese with English abstract).

Zhang, S. C., Wang, F. Y., Zhang, B. M., Liang, D. G., and Zhao, M. J. (2000). Middle-Upper Ordovician Source Rock Geochemistry of the Tarim Basin. *Acta Pet. Sin.* 21 (6), 23–28. (in Chinese with English abstract).

Zhang, S. C., ZhangBian, B. M. L. Z., Jin, Z. J., Wang, D. Y., Zhang, X. Y., Gao, Z. Y., et al. (2005). Development Constraints of Marine Sourcerocksin China. *Earth Sci. Front.* 12 (3), 39–48. (in Chinese with English abstract).

Zhang, S. C., Zhang, B. M., Li, B. L., Zhu, G., Su, J., and Wang, X. (2011). History of Hydrocarbon Accumulations Spanning Important Tectonic Phases in Marine Sedimentary Basins of China: Taking the Tarim Basin as an Example. *Development* 38 (1), 1–15. doi:10.1016/S1876-3804(11)60010-4

Zhang, S., Moldowan, J. M., Li, M., Bian, L., Zhang, B., Wang, F., et al. (2002b). The Abnormal Distribution of the Molecular Fossils in the Pre-cambrian and Cambrian: its Biological Significance. *Sci. China Ser. D-Earth Sci.* 45 (3), 193–200. doi:10.1360/02yd9021

Zhao, M. J., Qin, S. F., Pan, W. Q., Song, Y., Wang, Z., and Han, J. (2008a). The Hydrocarbon Source Analysis of Buried-Hill Reservoir of Ordovician in Western Lunnan Area of Tabei Uplift. *Xinjiang Pet. Geol.* (04), 478–481.

Zhao, M. J., Wang, Z. M., Pan, W. Q., Liu, S., Sheng, F., and Jian, H. (2008b). Lower Palaeozoic Source Rocks in Manjiaer Sag, Tarim Basin. *Petroleum Explor. Dev. Online* 35 (4), 417–423. doi:10.1016/s1876-3804(08)60089-0

Zhao, W. Z., Xie, Z. Y., Wang, X. M., Shen, A., Wei, G., and Wang, K. (2021). Sinian Gas Sources and Effectiveness of Primary Gas-Bearing System in Sichuan Basin,SW China. *Petroleum Explor. Dev.* 48 (6), 11. doi:10.1016/s1876-3804(21)60285-9

Zhu, G. Y., Liu, X. W., Zhu, Y. F., and Wang, K. (2013). The Characteristics and the Accumulation Mechanism of Complex Reservoirs in the Hanilcatam Area, Tarim Basin. *Bull. Mineralogy, Petrology Geochem.* 32 (02), 231–242. doi:10.11885/j.issn.1674-5086.2012.09.03.02

Zhu, G. Y., Yang, H. J., and Zhu, Y. F. (2011). Study on Petro-Leum Geological Characteristics and Accumulation of Carbonate Reser-Voirs in Halahatang area,Tarim Basin. *ActaP etrologica Sin.* 27 (3), 827–844.

Zhu, W. P., Sun, D., and Yao, Q. Z. (2021). The Law of Hydrocarbon Accumulation in Carbonate Reservoirs in Halahatang Area,Tarim Basin. *Special Oil Gas Reservoirs* 28 (02), 41–48.

**Conflict of Interest:** The authors declare that the research was conducted in the absence of any commercial or financial relationships that could be construed as a potential conflict of interest.

**Publisher's Note:** All claims expressed in this article are solely those of the authors and do not necessarily represent those of their affiliated organizations, or those of the publisher, the editors, and the reviewers. Any product that may be evaluated in this article, or claim that may be made by its manufacturer, is not guaranteed or endorsed by the publisher.